

# Evaluating the System Performance of a Pressure Swing Adsorption (PSA) Unit by Removing the Carbon Dioxide from Biogas

Antonio-Abdu Sami M. Magomnang<sup>1\*</sup>, Amado L. Maglinao Jr.<sup>2</sup>, Sergio C. Capareda<sup>2</sup> and Eliseo P. Villanueva<sup>3</sup>

<sup>1</sup>Mechanical Engineering Department, University of Science and Technology of Southern Philippines – CDO Campus, Lapasan, Cagayan de Oro City - 9000, Philippines; a\_magomnang@yahoo.com,

<sup>2</sup>Bio-Energy Testing and Analysis Laboratory, Biological and Agricultural Engineering Department, Texas A & M University, College Station, Texas - 77843, United States of America; amado\_jr@tamu.edu, scapareda@tamu.edu

<sup>3</sup>Mechanical Engineering Department, Mindanao State University – Iligan Institute of Technology, Tibanga, Iligan City - 9200, Philippines; ep\_villanueva@yahoo.com

## Abstract

**Objectives:** This study aims to assess the performance of a Pressure Swing Adsorption (PSA) unit in removing the carbon dioxide from biogas by evaluating the breakthrough and adsorption capacity of the adsorption process as well as determining the effects of cyclic regeneration of the adsorbent. **Methods:** The PSA system was developed in order to establish the behavior of different gas separation experiments. It can be operated up to 10 bars pressure at ambient temperatures and gas flow rate from 0 to 15 L min<sup>-1</sup>. It is composed only of one main vessel made up of 316 stainless steel components. Use of physical adsorbent (Zeolite 13X) in a Pressure Swing Adsorption (PSA) system will consume the gaseous impurities such as CO<sub>2</sub>. Product gas was collected into 1 L Tedlar bags and analyzed using SRI gas chromatograph with TCD and HID detector to validate the CO<sub>2</sub> and CH<sub>4</sub> composition. **Findings:** The results of the Pressure Swing Adsorption (PSA) experiments showed an average increase of 160% in the net heating value over that of a certified gas standard. The amount of methane was also significantly higher although the amount of the other gasses (i.e. nitrogen) remained comparatively the same. The number of other gases was significantly lower and no trace of carbon dioxide was observed in the PSA product gas indicating that carbon dioxide had been completely absorbed by the system. **Application:** This study helps to reduce CO<sub>2</sub> emitted to the atmosphere from the anaerobic co-digestion of biogas to produce high energy content bio-methane fuel.

**Keywords:** Adsorption, Biogas, Carbon Dioxide, Methane Gas, Pressure Swing Adsorption, Zeolite 13X

## 1. Introduction

Biogas is a renewable, high-quality fuel which can be produced from various organic raw materials and used for various energy services. Biogas technology has been

developed and widely used over the world because it has several advantages – the reduction of the dependence on non-renewable resources, high energy-efficiency, environmental benefits, available and cheap resources to feedstock, relatively easy and cheap technology for pro-

\*Author for correspondence

duction, and extra values of dig estate as a fertilizer. But the current status of biogas production and utilization varies largely among continents. Biogas as a renewable source of energy is becoming increasingly important since biogas has some ecological advantages mainly being CO<sub>2</sub> neutral; hence, it reduces the formation of greenhouse gases. Furthermore, biogas represents a meaningful way of both waste use and waste disposal as agricultural, commercial and municipal waste from biogenic sources used for the production of different types of biogas. The main components of biogas are methane (CH<sub>4</sub>) and Carbon Dioxide (CO<sub>2</sub>); it also contains significant quantities of undesirable compounds. Table 1 shows the typical compounds and their concentrations in a biogas. For the exploitation of energy gained from biogas, the amount of methane is essential: the higher the amount of methane, the higher the output of energy from biogas. The other components are mostly useless for the energy production such as nitrogen or water. It is even possible that a negative impact on engine reliability can be provoked by trace components such as Hydrogen Sulfide (H<sub>2</sub>S), Ammonia (NH<sub>3</sub>) and Siloxanes. The trace components can be very harmful as the aggressive substances formed may destroy the engine, e.g., due to corrosion<sup>1,2</sup>. There have been many

methods to reduce carbon dioxide emissions in the form of CO<sub>2</sub> capture and storage, for example, through its injection into underground waters, saline waters or aquifers in which, CO<sub>2</sub> is transferred from one place to another. With this approach, there is always the risk of CO<sub>2</sub> release to the environment. However, these technologies available for removal of CO<sub>2</sub> from biogas are typically used for larger scale applications such as upgrading natural gas from “sour” gas wells, sewage treatment plants, and landfills. Because of the different contaminants, scales, and applications, removal of CO<sub>2</sub> from dairy manure biogas will differ significantly from these applications and requires a case-by-case analysis. The following processes can be considered for CO<sub>2</sub> removal from biogas as presented in Table 2. The processes are presented roughly in the order of their current availability for and applicability to dairy biogas upgrading. With regards to the carbon dioxide removal, several and well-established methods are commonly carried out such as water scrubbing, chemical absorption, pressure swing adsorption, member separation and cryogenic process, as presented and summarized in Table 2.

A Pressure Swing Adsorption (PSA) processes separate out CO<sub>2</sub>, oxygen and nitrogen by absorption and desorption on activated carbon at different pressures in four stages - adsorption, depressurizing, desorption and pressure build up. The principle of the pressurized process uses the fact that gases like carbon dioxide are more readily dissolved in activated carbon than methane. The biogas upgrading plant consists of a scrubber vessel for scrubbing (absorption of CO<sub>2</sub> into adsorbent like activated carbon), a flash tank for methane gas recovery, and a desorption tower for the regeneration. The pressure swing adsorption method of CO<sub>2</sub> removal was chosen because of its capability of its material presents stronger surface interactions to CO<sub>2</sub>, to adsorb larger loadings as compared to methane<sup>3</sup>. Aside from that, it is a promising option to separate CO<sub>2</sub> due to its ease of applicability over a wide range of temperature and pressure conditions, its low energy requirements and its low capital invest-

**Table 1.** Typical components of a biogas<sup>1</sup>

| Component        | Concentration |
|------------------|---------------|
| Methane          | 40 – 75%      |
| Carbon Dioxide   | 25 – 55%      |
| Water (Steam)    | 0 – 10%       |
| Nitrogen         | 0 – 5%        |
| Oxygen           | 0 – 2%        |
| Hydrogen         | 0 – 1%        |
| Hydrogen Sulfide | 0 – 1%        |
| Ammonia          | 0 – 1%        |

**Table 2.** Summary of the technologies for the Carbon Dioxide removal<sup>5</sup>

| Parameters                           | Methods         |                     |                           |                     |           |
|--------------------------------------|-----------------|---------------------|---------------------------|---------------------|-----------|
|                                      | Water Scrubbing | Chemical absorption | Pressure swing adsorption | Membrane separation | Cryogenic |
| Gas Pre-Cleaning Requirement         | No              | Yes                 | Yes                       | Yes                 | Yes       |
| Working Pressure                     | 9 - 10 Bar      | 1 Bar               | 4 - 7 Bar                 | 4 - 7 Bar           | 40 Bar    |
| Methane Loss                         | 1 - 2%          | 1 - 2%              | 1 - 9%                    | 10 - 15%            | 1 - 2%    |
| % purity attained of upgraded biogas | 95 - 98%        | Up to 99%           | 95 - 99%                  | Up to 90%           | Up to 99% |
| Heat Requirement                     | -               | Required            | -                         | -                   | -         |
| Operating Cost                       | Low             | Moderate            | Moderate                  | Low                 | High      |
| Initial Cost                         | Low             | Moderate            | Moderate                  | Moderate            | High      |
| Process Handling                     | Easy            | Complex             | Easy                      | Easy                | Complex   |

ment<sup>4</sup>. After upgrading, the gas then is used for possible engine testing in a stationary non-road engine. In order to overcome the problem in increasing the methane recovery from upgrading, this study aims to Assess the performance of a Pressure Swing Adsorption (PSA) unit in removing the carbon dioxide from biogas by evaluating the breakthrough and adsorption capacity of the adsorption process as well as determining the effects of cyclic regeneration of the adsorbent from the anaerobic co-digestion of agricultural biomass waste utilizing dairy manure co-digested with various biomass feedstock's for power generation applications.

## 2. Materials and Methods

### 2.1 Carbon Dioxide Upgrading using Pressure Swing Adsorption (PSA)

The Pressure Swing Adsorption (PSA) system was used to

upgrade the biogas produced from anaerobic co-digestion of cattle manure with sewage sludge, rice straw, and coconut shell. Before the conduct of the experiments as shown in Figure 1, the system was first developed and installs instruments for monitoring and control. The PSA system was developed in order to establish the behavior of different gas separation experiments. It can be operated up to 10 bars pressure at ambient temperatures and gas flow rate from 0 to 15 L min<sup>-1</sup>. It is composed only of one main vessel made up of 316 stainless steel components with a flange for adsorbent replacement as shown in Figure 2. The vessels have 43 ft<sup>3</sup> of volume for the adsorbent bed such as zeolites, activated carbon, and carbon molecular sieves. For this research, DeLSORB® 13X812B molecular sieve (Delta Adsorbents, USA) was used as an adsorbent. Its specifications and properties are given in Table 3 and 4. This adsorbent is best suitable for carbon dioxide removal from biogas.

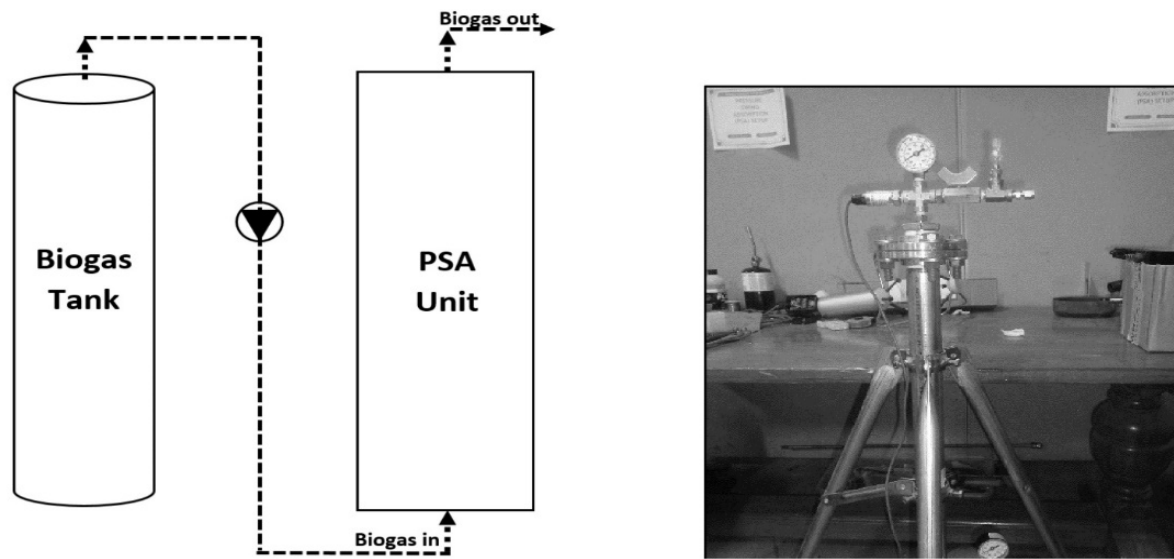


**Figure 1.** Schematic diagram of the pressure swing adsorption system. (a) PSA adsorption (Schematic) (b) PSA adsorption (Actual)

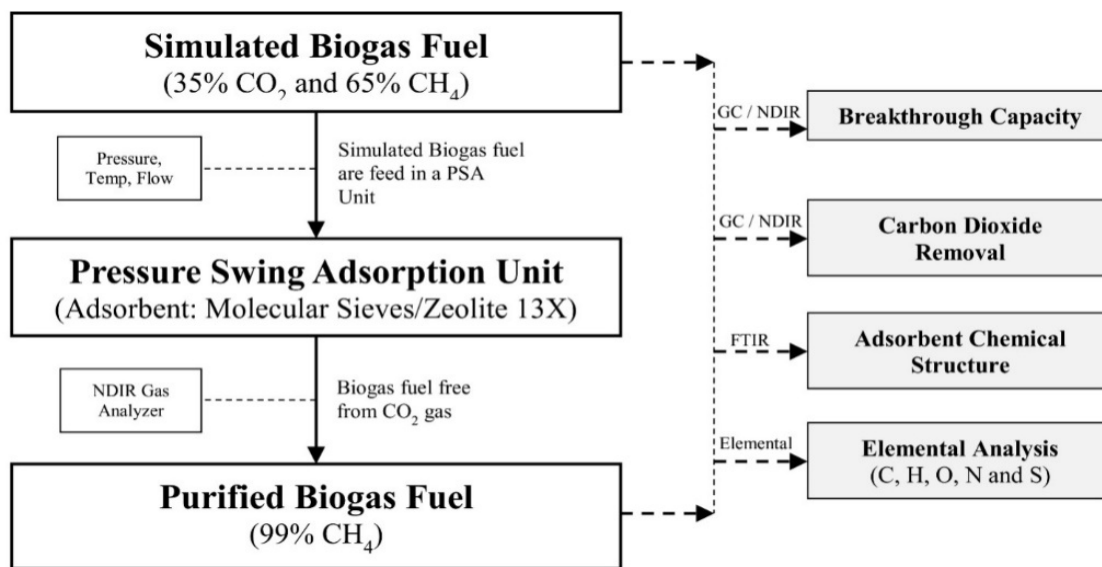


**Figure 2.** Schematic diagram of the pressure swing adsorption experimental procedure conducted in this study.

## 2.2 Biogas Upgrading Experimental Conditions

The experimental set-up is created for the removal of carbon dioxide from the biogas. Wherein, the surrogated gas mixture comprised of 63.18% vol.  $\text{CH}_4$  and 36.82 %vol.  $\text{CO}_2$  will be passing through the adsorbent bed in an up-flow motion and pure methane in a down-flow motion

in order to regenerate the adsorbent<sup>6</sup>. For this study, we will compare the effects on the adsorption of using Zeolite (Molecular Sieve) 13X as an adsorbent for the removal of  $\text{CO}_2$  from biogas. The experiments were conducted using a certified gas mixture standard prepared by Airgas (Airgas Southwest, Woodlands TX). This gas mixture is a good representation of the biogas produced from anaerobic co-

digestion processes. For this experiment, the pressure was set at 10 psi, 20 psi and 35 psi and the product gas outlet flow rate at 0.5 LPM. Product gas was collected into 1 L Tedlar bags (Restek, Bellefonte, PA) and analyzed using SRI gas chromatograph (SRI Instruments, Torrance, CA) with TCD and HID detector to validate the  $\text{CO}_2$  and  $\text{CH}_4$  composition. Also, the pressure was set at 400 kPa and the product gas outlet flow rate at 0.5-1.0 LPM. Product gas was collected into 1 L Tedlar bags (Restek, Bellefonte, PA) and analyzed using SRI gas chromatograph (SRI Instruments, Torrance, CA) with TCD and HID detector to validate the  $\text{CO}_2$  and  $\text{CH}_4$  composition. The product gas was also analyzed in real time using the Horiba NDIR gas analyzer.

### 2.3 Characterization of the Adsorbent using FTIR

The characterization was done for the adsorbed zeolite 13X in comparison with new zeolite 13X. The Fourier Transform Infrared Radiation (FTIR) analysis was conducted using Fourier Transform Infrared (FTIR) spectroscopy (Shimadzu, IR Affinity-1 with MIRacle universal sampling accessory). The infrared spectra were collected in a range of  $4000\text{--}600\text{ cm}^{-1}$  with a resolution of  $4\text{ cm}^{-1}$ .

### 2.4 $\text{CO}_2$ Adsorption Studies

Pressure Swing Adsorption (PSA), working between high pressure level during adsorption and a low-pressure level for desorption<sup>7</sup> employed the most basic sequence of steps, referred to as the skarkstorm cycle, consist of pressurization of adsorber bed by the feed gas followed by adsorption and depressurization (blown down) followed by a purge or evacuation of the highly adsorbed component. The simple skarkstorm four-step cycle was selected for baseline analysis for this research because of the simplicity of the processes. The removal of carbon dioxide with PSA beds packed with zeolite 13X as an adsorbent and operated with four steps: pressurization, adsorption, depressurization, and desorption. During the pressurization step, high-pressure feed gas representing the biogas composition consisting of 63.18%  $\text{CH}_4$  and 36.82%  $\text{CO}_2$  at

ambient temperature is supplied to the bottom of the bed. During the adsorption step,  $\text{CO}_2$  is adsorbed on a fixed adsorbent (zeolite 13X);  $\text{CH}_4$  is obtained as a product at the top of the bed, and the high-pressure feed gas enters the bed continuously as in the pressurization step. During the depressurization step,  $\text{CO}_2$  starts being recovered. The desorption step at the bottom of the bed and air at ambient pressure is employed as a purge gas.

During the experiment, a list of key assumptions relevant to the PSA model:

- All steps are assumed to operate in batch mode.
- A batch system consists of a vessel with a fixed volume.
- Equilibrium exists between two homogeneous phases: the bulk gas in the adsorbent voids and the adsorbed gas on the surface of the adsorbent.
- The desorbed bed does not contain residual component gas.
- The adsorption is adiabatic.

#### 2.4.1 Breakthrough Experiments

The breakthrough curve plotted under reduced coordinates (ratio of the outlet to the feed molar fraction) as reported in Figure 1. For simplicity, a binary gas mixture of 63.18%  $\text{CH}_4$  and 36.82%  $\text{CO}_2$  represented in a typical biogas composition is assumed in this analysis.

#### 2.4.2 Regeneration and Reusability of the Zeolite 13X at Room Temperature

Out of the adsorbent studied, zeolite 13X showed the best adsorption capacity at  $30^\circ\text{C}$ . Therefore, it was studied for reusability with free-flowing air desorption at room temperature in the same run followed by vacuum purge. It was seen that the adsorbent successfully retained adsorption capacity in three consecutive reuse cycles. There is a slight loss of capacity after the first cycle probably owing

to some irreversible adsorption of the first cycle that could have been desorbed at room temperature.

### 2.4.3 C, H, N, and S Content (Elemental) Analysis Content after Repeated Cycles of Adsorption

In order to confirm the stability of the zeolite 13X, particularly the stability of the adsorbent on the regeneration by vacuum, purge air, and drying on the zeolite matrix, adsorption cycles were repeated three (3) times. C, H, N and S analysis was carried using the elemental analyzer (Vario MICRO cube, Elementar, NJ, USA).

### 2.4.4 Selectivity Studies

The carbon dioxide selectivity of the adsorbents was studied using a representative binary mixture of 63.18% vol. CH<sub>4</sub> and 36.82% vol. CO<sub>2</sub> of biogas prepared by setting the flows around 0.63 liters/min. prior to the adsorbent study, the adsorbent was pre-weighted and placed in the PSA unit. The binary mixture was then passed over the adsorbent, and the outlet was continuously monitored by Horiba NDIR gas analyzer. In the results, since CO<sub>2</sub> breakthrough occurred early, only the saturation capacities are compared, that is, till the total adsorption capacity of the adsorbent was used up.

## 2.5 Implemented Pressure Swing Adsorption (PSA) System Set-up

Figure 3 shows the schematic diagram of how the developed PSA system works. The raw gas mixture enters the bottom of the reactor with its flow being controlled by the valve from the gas supply tank. The valves divert the raw gas mixture into the active vessel. It is pressurized to the set pressure (i.e. 400 kPa) and when reached, the outlet valve is partially open to allow the flow of the product gas. The pressure inside is maintained at the desired value by controlling the flow rate of the product gas. The valves are then continuously opened after the adsorption cycle is finished to allow the gases evacuate from the vessel (reactor column). After evacuation, the reactor regenerates as the pressure decreases to atmospheric pressure through a vent or by directing it to a vacuum pump. Adsorption

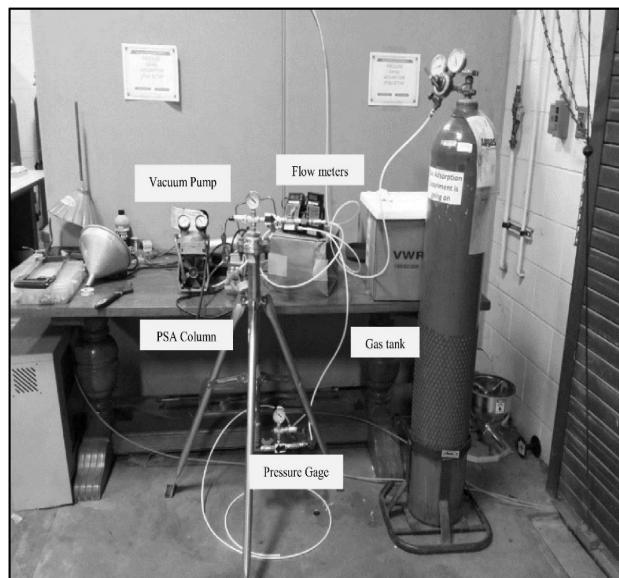


**Figure 3.** Biogas upgrading (pressure swing adsorption) experimental set-up.

in the vessel again completes the cycle and this process repeats to have a nearly continuous gas production.

## 2.6 PSA Adsorption Experiments

During the pressurization stage, the raw gas inlet flow rate started at 1.7 LPM and ended at around 1.28 LPM until the vessel was desorbed. The performance of the PSA system based on the product gas composition will be based on the selectivity of the adsorbent and amount adsorbed with respect to the molecular sieve/zeolite 13X. The desired concentration of the product gas was achieved in a short span of 90 seconds during adsorption. Each adsorption cycle increases the methane concentration to an average of 63% respectively and decreases the amount of carbon dioxide up to 99.9%. A longer stable gas concentration may be achieved by using more adsorbent. As the adsorbent became saturated early, using a larger scale PSA system could address the problem. Thus, the use of the PSA system presents a feasible application to producing a cleaner biogas and reducing the problems in downstream operations.

The PSA experiments using the biogas from anaerobic digestion showed an average increase of 160% in the gas net heating value compared with the certified gas stan-

standard shown in Table 5. Further, the amount of carbon dioxide was observed in the PSA product gas indicating that carbon dioxide had not been completely absorbed by the system. For this experiment, the pressure was set at 400 kPa and the product gas outlet flow rate set at 1.63 LPM (Table 5). Product gas was collected into 1 L Tedlar bags (Restek, Bellefonte, PA) and analyzed using SRI gas chromatograph (SRI Instruments, Torrance, CA) with TCD and HID detector to validate the CO<sub>2</sub> and CH<sub>4</sub> composition. The product gas was also analyzed in real time using the Horiba NDIR gas analyzer.

## 3. Results and Discussion

### 3.1 CO<sub>2</sub> Upgrading System Evaluation

#### 3.1.1 Breakthrough Experiments

Adsorption is a transient process and the amounts of material adsorbed within a fixed bed will depend on both position and time. The CO<sub>2</sub> breakthrough curves for the zeolite 13X is shown in Figure 4, and the experimental conditions are given in Table 3 & 4. For simplicity, a binary gas mixture of 63.18% vol. CH<sub>4</sub> and 36.82% vol. CO<sub>2</sub> rep-

**Table 3.** Properties of molecular sieves

| Parameters                                       | Values   |
|--|--|
| Name   | Molecular Sieve Type 13X   |
| Chemical Formula                                 | SiO <sub>2</sub> , Na <sub>2</sub> O, Al <sub>2</sub> O <sub>3</sub> , MgO |
| BET Surface area (m <sup>2</sup> /g)             | 279.912  |
| Average Pore Radius (Å)                          | 9.33309  |
| Bulk Density (kg/m <sup>3</sup> )                | 45   |
| Particle Diameter (mm)                           | 1.5875   |
| Pore Volume (cc/g) at P/P <sub>0</sub> = 0.35006 | 0.1306   |
| Appearance                                       | Pellets  |
| Adsorbent Shape                                  | Cylindrical  |

**Table 4.** Experimental conditions in the PSA upgrading

| Parameters                   | Values  |
|------------------------------|---|
| Adsorbent Vessel material    | 316 Stainless Steel                               |
| Bed Volume (m <sup>3</sup> ) | 1.21762   |
| Reactor length (m)           | 0.6604 (26 in)                                    |
| Reactor diameter (m)         | 0.040894 (1.61 in)                                |
| Gas Phase Composition        | 35% vol CO <sub>2</sub> , 65% vol CH <sub>4</sub> |

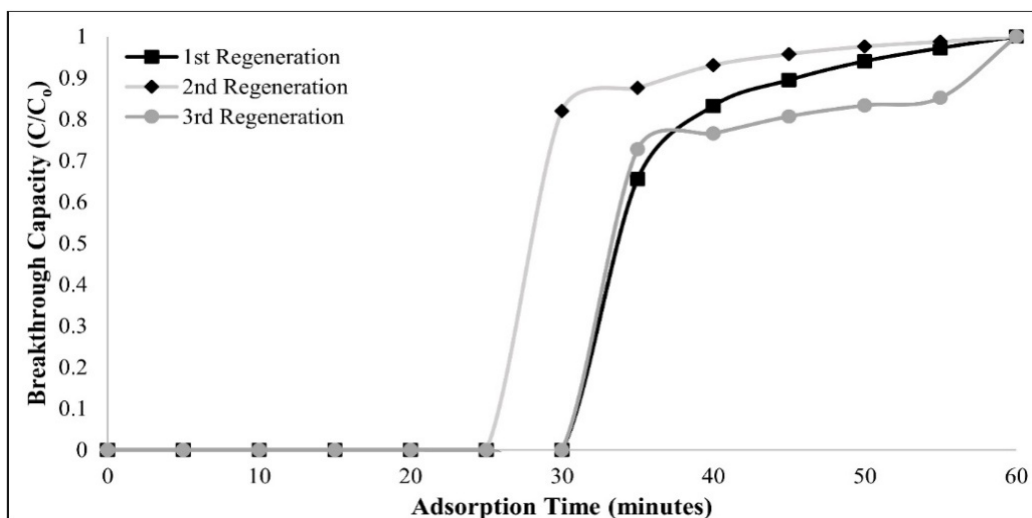


Figure 4. Breakthrough curve for CO<sub>2</sub> removal using zeolite 13X at 400 kPa pressure.

resented in a typical biogas composition is assumed in this analysis.

The breakthrough curves show the ratio of the outlet concentration and the influent concentration against the contact time at an atmospheric pressure, and at some temperatures. The general pattern of the breakthrough curves was achieved as expected for all adsorbents. For zeolite 13X, the adsorption breakthrough around 25–35 minutes depending on the efficiency of desorption (regeneration) of the adsorbent. This shows that the pore diameter of zeolite 13X (10 Å) is sufficient for the CO<sub>2</sub> to enter into the zeolites channels. The major cations of zeolites are Na and K and this major cation appears to play the main role in the adsorption of CO<sub>2</sub>. Also, sodium appears to be the

favorable cation for the adsorption of CO<sub>2</sub>. The saturation time for zeolite 13X is longer due to the larger pore volume. Also, the differences in adsorption observed with zeolites should be related to the differences in the chemical nature of the surface and porosity. The zeolites have higher surface area than other adsorbent and that may have contributed to the higher adsorption capacity of zeolites. The reported values of carbon dioxide adsorption are in agreement with the previously published data, although the reported values of amount adsorbed are higher than all previous literature. In low-pressure range, the amount adsorbed compares very well with the data reported<sup>4</sup>.

Table 5. PSA adsorption experimental conditions for biogas upgrading

| Runs | Outside Temp | Pressure (feed) | Pressure (equalization) | Time (pressurization) | Time (adsorption) | Flow rate (in) | Flow Rate (out) |
|------|--------------|-----------------|-------------------------|-----------------------|-------------------|----------------|-----------------|
|      | (°C)         | (kpa)           | (kpa)                   | (min)                 | (min)             | L/min          | L/min           |
| 1    | 22.0         | 400             | 400                     | 3.00                  | 63.40             | 1.63           | 0.82            |
| 2    | 19.6         | 400             | 400                     | 3.60                  | 63.27             | 1.63           | 0.77            |
| 3    | 19.1         | 400             | 400                     | 2.43                  | 63.27             | 1.48           | 0.77            |

### 3.1.2 Effects of Cyclic Regeneration of Adsorbents

Using the Pressure Swing Adsorption (PSA) system, an experiment was begun by regenerating the zeolite 13X adsorbent in the muffle furnace at 315°C under standard atmospheric and pressure conditions over the 24-hr period. Then, the desired amount of surrogated biogas mixture (63.18% vol. CH<sub>4</sub> and 36.82% vol. CO<sub>2</sub>) was injected into the PSA system, and the flow rate was fixed for the initial equilibration.

Then, the gas phase concentration of the PSA system was measured using the Horiba NDIR gas detector and

further validated by SRI gas chromatograph. The pressure was held constant until equilibrium was established as determined by sampling the gas phase. The measurements were continued until the breakthrough was reached. After adsorption experiment, a regeneration of the adsorbent will be done by flowing countercurrent atmospheric air to the PSA system to desorb the CO<sub>2</sub> from the system. The adsorption capacity of the zeolite 13X indicates the reusability (regeneration capacity) of the adsorbent as presented in Figures 5 and 6. Based on the experimental results, a 100% removal of carbon dioxide from the

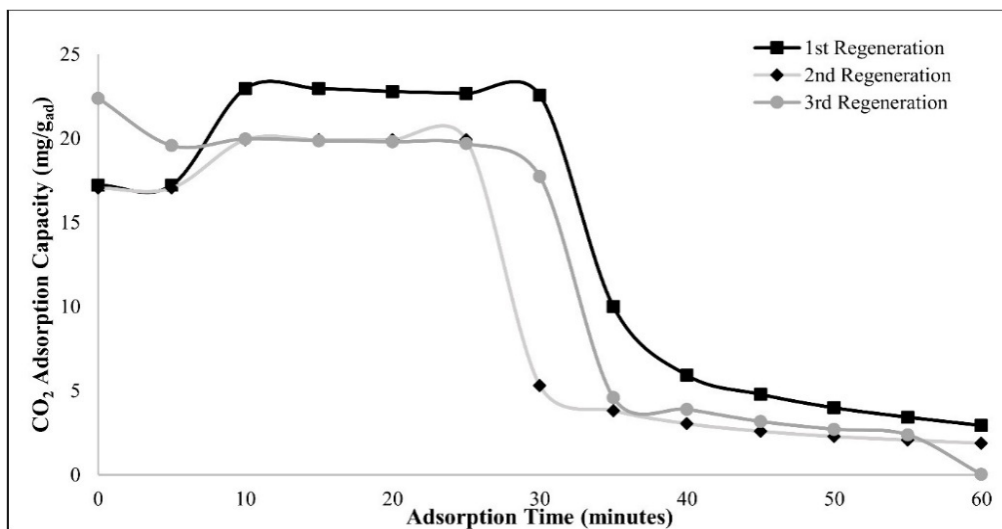


Figure 5. Adsorption isotherms for CO<sub>2</sub> sorption into zeolite 13X at 0 psi.

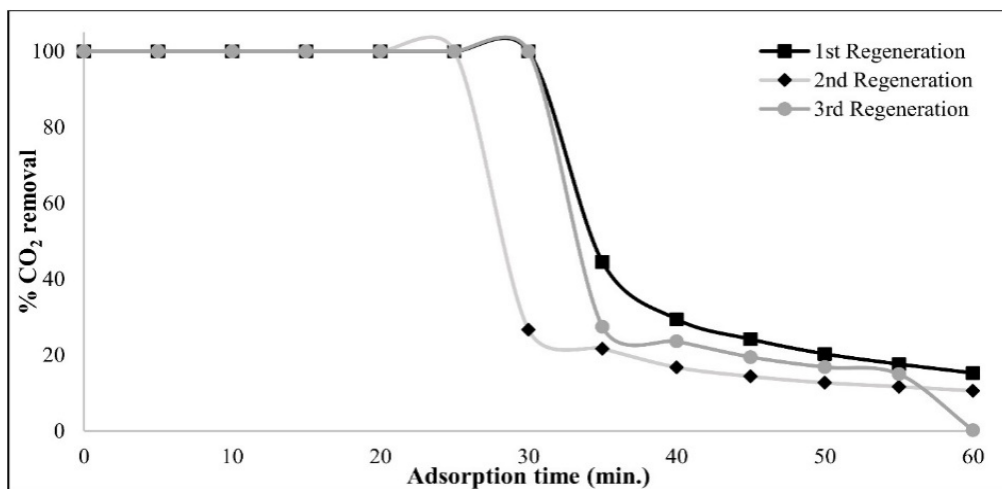


Figure 6. Percentage removal of CO<sub>2</sub> sorption at different regeneration cycles.

biogas is maintained after some time and the zeolite can be reused by passing through a countercurrent flow of air. However, removal (desorption) efficiency of zeolite decreases every time it regenerates and it implied that the zeolite is not completely regenerated by air. This issue will be addressed by introducing hot air during the regeneration process.

### 3.1.3 Adsorption Kinetics and Contact Time Studies

Kinetic parameters of an adsorption process are essential for the evaluation of adsorption parameters, which in turn control the entire process of sorption, which is important for designing sorption systems.

Three repeated cycles of CO<sub>2</sub> adsorption and desorption (regeneration) using Zeolite 13X were performed in

this study. The system characteristics, shown in Table 6, were kept constant throughout all three cycles. The results of multiple cycles of adsorption and desorption using Zeolite 13X are shown in Figures 7 and 8 and Table 7. The adsorption curves observed in this study for Zeolite 13X (Figure 7) are similar to those observed<sup>8</sup>.

Upon the introduction of the CO<sub>2</sub>-CH<sub>4</sub> gas mixture to molecular sieve 13X, the effluent concentration dropped to 0 ppm<sub>v</sub> for approximately 26-33 min. The initial capacity is 22.5 g<sub>CO<sub>2</sub></sub>/kg<sub>Zeolite13X</sub>, and is slightly lower than the reported values of <sup>9</sup>for a gas mixture containing N<sub>2</sub> (75%) and CO<sub>2</sub> (25%). This is expected because the gas mixture is different (63.18% CH<sub>4</sub> and 36.82% CO<sub>2</sub>) and also, the adsorption step in this experiment was terminated before complete saturation could be achieved. Figure 6 also shows that the time to reach the saturation capac-

**Table 6.** Summary of experimental results on the CO<sub>2</sub> upgrading from biogas

| Experimental run | P (kPa) | flow out (Lpm) | t <sub>break</sub> (min) | q <sub>sat</sub> (mg/g <sub>ads</sub> ) |
|------------------|---------|----------------|--------------------------|---|
| 1st Regeneration | 400     | 0.87           | 33.56                    | 22.50                                   |
| 2nd Regeneration | 400     | 0.78           | 26.33                    | 19.92                                   |
| 3rd Regeneration | 400     | 0.77           | 30.60                    | 17.74                                   |

**Table 7.** Certified gas standard chromatograph results

| Component                    | Certified Std. Values | GC Value |
|------------------------------|-----------------------|----------|
| Methane (% vol.)             | 64.2                  | 63.2     |
| Carbon Dioxide (% vol.)      | 35.8                  | 36.8     |
| Net calorific value* (MJ/kg) | 19.78                 | 19.1     |

\* Net calorific value is calculated using this website "<http://unitrove.com/engineering/tools/gas/natural-gas-calorific-value>", and it is compliant with accordance to ISO 6976 (1995) Natural gas - Calculation of calorific values, density, relative density and Wobbe index from composition.

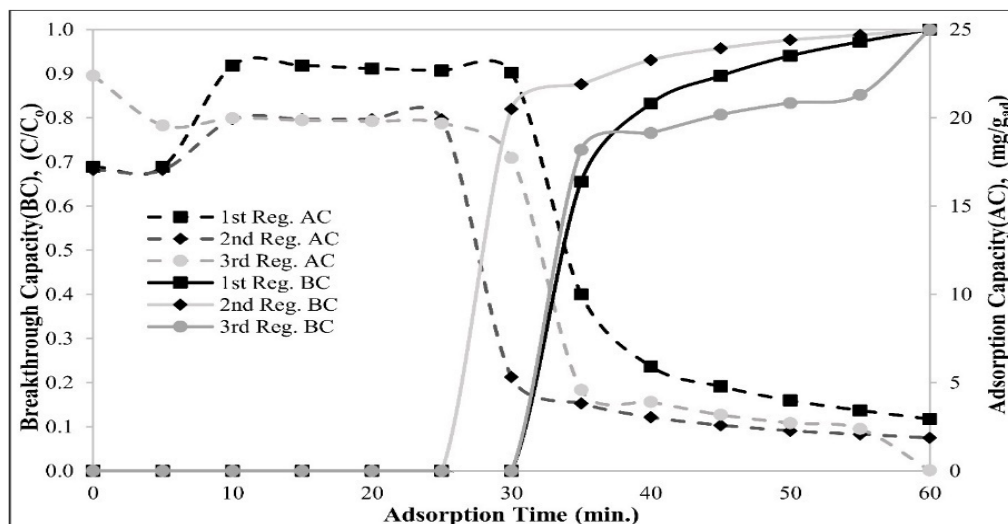


**Figure 7.** Consolidated CO<sub>2</sub> sorption isotherms of breakthrough and adsorption capacity at different regeneration cycles.

ity decreases with each successive cycle. This behavior is attributed to a residual of CO<sub>2</sub> that was not removed from the adsorbent during the desorption (regeneration) period.

The adsorption isotherms for repeated cycles were very similar as shown in Figure 7. This indicated that the adsorption is fully reversible and complete regeneration can be obtained by evacuation of the material after adsorption. The final adsorption isotherm (3<sup>rd</sup> Regeneration which was obtained after the completion of adsorption experiments with CH<sub>4</sub>) was conducted with CO<sub>2</sub> and it was very similar to the previous adsorption isotherms with CO<sub>2</sub>. This indicated that the sorbent was not affected by the adsorption of CH<sub>4</sub>.

After the introduction of the gas mix to the molecular sieve 13X, the CO<sub>2</sub> concentration decreased to almost zero while the methane concentration increased to 100%, until the breakthrough. This indicates that an excellent separation of CO<sub>2</sub> from a gas mixture of CH<sub>4</sub> and CO<sub>2</sub> can be obtained with molecular sieve 13X.

Furthermore, the percentage removal of carbon dioxide by molecular sieve/zeolite 13X is shown as a function of adsorption time is shown in Figure 6. These values were determined using Equation 1, where C<sub>i</sub> and C<sub>f</sub> are the initial and the final concentrations, respectively, of

carbon dioxide adsorbed in the system, both of which were determined by NDIR gas analyzer and validated by SRI gas chromatograph.

$$\text{Percentage removal} = \left[ \frac{C_i - C_f}{C_i} \right] \times 100 \quad (1)$$

In addition, the results show that the extent of carbon dioxide removal by the molecular sieve/zeolite 13X adsorbent initially increases with the increase in contact time and reaches the equilibrium where it showed the maximum removal.

The removal of carbon dioxide maintained the equilibrium point until 26, 30 and 33 min, respectively, and these three-time periods were thus considered as the optimum adsorption times for each carbon dioxide species.

Therefore, the adsorption capacity of zeolite 13X at various regeneration cycles are shown in Figure 8, is able to remove significant amounts of carbon dioxide more rapidly than by many other regeneration cycles with same adsorbents. Further, the unused adsorbent is more efficient for carbon dioxide removal in terms of equilibration time and removal capacity. It shows that adsorption using the zeolite 13X shows a competitive performance with other adsorbents at various regeneration cycles. The

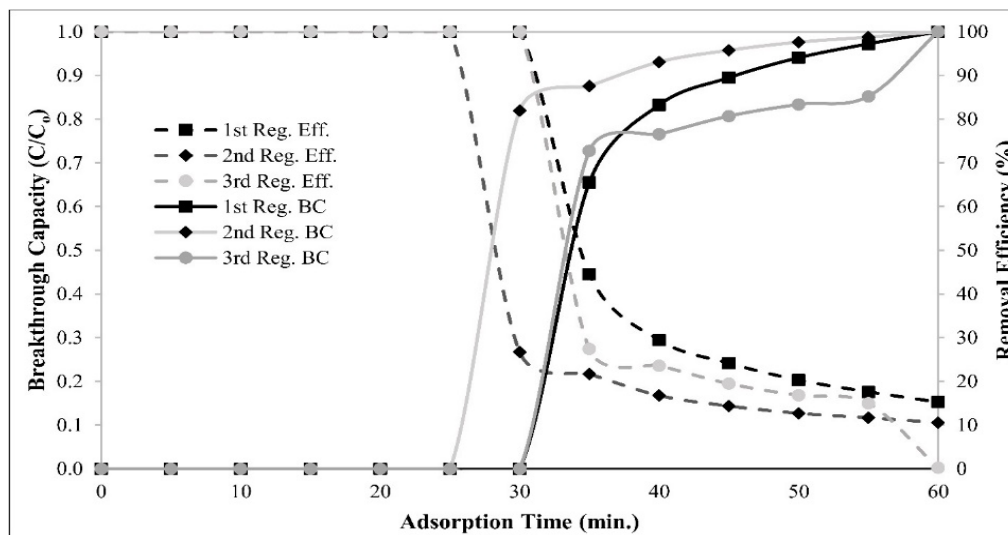


**Figure 8.** Consolidated CO<sub>2</sub> sorption isotherms of breakthrough capacity and removal efficiency at different regeneration cycles.

percentage removal of carbon dioxide ions increased with the increase of the regeneration/desorption (Figure 8). This increase in adsorption with the increase in the regeneration/desorption cycles is due to a higher surface area available for regeneration<sup>8</sup>.

### 3.1.4 Selectivity Study

The carbon dioxide selectivity of the adsorbents was studied using a representative binary mixture of 63.18% vol. CH<sub>4</sub> and 36.82% vol. CO<sub>2</sub> of biogas prepared by setting the flows around 0.8 liters/min. prior to the adsorbent study, the adsorbent was pre-weighted and placed in the PSA unit. The binary mixture was then passed over the adsorbent, and the outlet was continuously monitored by Horiba NDIR gas analyzer. In the results, since CO<sub>2</sub> breakthrough occurred early, only the saturation capacities are compared, that is until the total adsorption capacity of the adsorbent was used up.

As reported by many studies, the adsorption capacity of the zeolite 13X is found to be higher for CO<sub>2</sub> than for CH<sub>4</sub><sup>10</sup>. The saturation adsorption capacities of Zeolite 13X for CO<sub>2</sub> and CH<sub>4</sub> are (22.50, 19.92 and 17.74 mg/g<sub>ads</sub>) respectively.

Thus, the breakthrough for CH<sub>4</sub> shows a hump (C/Co > 1). This is the typical nature of a breakthrough curve

where competitive adsorption is taking place<sup>11</sup>. Initially, CH<sub>4</sub> being in higher concentration occupies more sites. With time, kinetic selectivity for CO<sub>2</sub> plays a role, and the adsorbed CH<sub>4</sub> is displaced making space for CO<sub>2</sub>. Thus, the outlet concentration of CH<sub>4</sub> shows a hump of concentration over than in the feed.

## 3.2 Characterization of Adsorbent used in the PSA Experiments

### 3.2.1 FT-IR Analysis of the Adsorbent before Desorption (Regeneration)

To determine the types of functional groups responsible for the removal of carbon dioxide species from the molecular sieve/zeolite 13X adsorbent, FT-IR analysis was performed on the adsorbent before and after the sorption process.

The FT-IR spectrum of the adsorbent shown in Figure 9 displays a number of vibration bands, indicating the complex nature of the adsorbent. Table 8 shows the changes in the major peak positions in the FT-IR spectrum of the adsorbent, before and after contact with CH<sub>4</sub>/CO<sub>2</sub> gas mixtures.

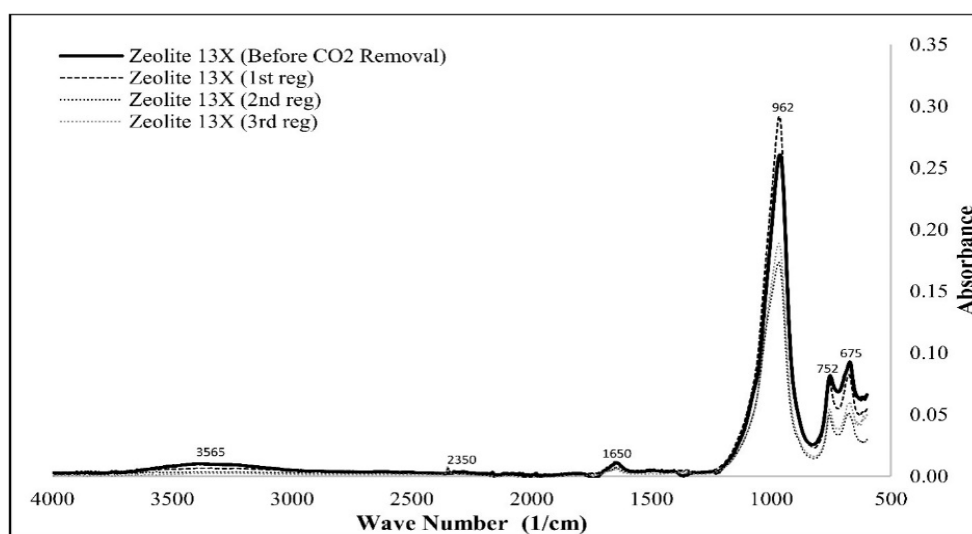
The spectra of molecular sieve/zeolite 13X adsorbents, after its regeneration cycles/stages, are shown in Figure 9.

**Table 8.** FT-IR spectral bands in the molecular sieve/zeolite 13X before and after contact with CH<sub>4</sub>/CO<sub>2</sub> gas mixtures

| FTIR band wavenumber (cm <sup>-1</sup> ) |               |               |               | Functional Groups Assignment                          | Reference           |
|--|---------------|---------------|---------------|---|---------------------|
| Before CO <sub>2</sub> Removal           | After 1st Reg | After 2nd Reg | After 3rd Reg |   |                     |
| 671                                      | 675           | 675           | 671           | Aromatic C-H Bending                                  | IR Absorption Table |
| 752                                      | 756           | 756           | 754           | Aromatic C-H Bending                                  | IR Absorption Table |
| 962                                      | 964           | 968           | 968           | vibrational stretching C-O, C=C, C-C-O                | IR Absorption Table |
| 1651                                     | 1645          | 1647          | 1649          | Conjugated carbonyl (amide), C=O Stretch              | In <sup>12</sup>    |
| 2350                                     | 2350          | 2349          | 2349          | Asymmetric OCO stretching of CO <sub>2</sub> gas      | In <sup>12</sup>    |
| 3564                                     | 3564          | 3566          | 3566          | O-H Stretching of water (3700-3050 cm <sup>-1</sup> ) | In <sup>12</sup>    |

The spectrum of the adsorbent shows, in the OH stretching region, weak sharp bands at 3735, 3675 and 3640

cm<sup>-1</sup> associated with residual hydroxyl groups and traces of adsorbed water molecules. After contact with water

**Figure 9.** FT-IR spectra of the molecular sieve/zeolite 13X adsorbent before and after contact with CO<sub>2</sub>/CH<sub>4</sub> gas mixture.

vapor, the scissoring mode of molecular water appears quite strong near  $1650\text{ cm}^{-1}$ , while the absorption goes to saturation in the region of OH stretching of water ( $3700\text{--}3050\text{ cm}^{-1}$ ).

Also, the spectrum of the surface of 13X molecular sieve shows a broad band centered at  $3365\text{ cm}^{-1}$ , a sharper component at  $2350\text{ cm}^{-1}$  and a sharp band at  $1650\text{ cm}^{-1}$ ,

due to stretching and scissoring modes of adsorbed water. The spectrum of zeolite 13X still presents weak features of residual strongly adsorbed water at  $3450$ ,  $3425$ ,  $3280$  and  $1665\text{ cm}^{-1}$ , together with hydroxyl groups adsorbing at absorbing at  $3755$ ,  $3735$  and  $3675\text{ cm}^{-1}$  weak and sharp. This spectrum compares with those recently presented<sup>13</sup>.

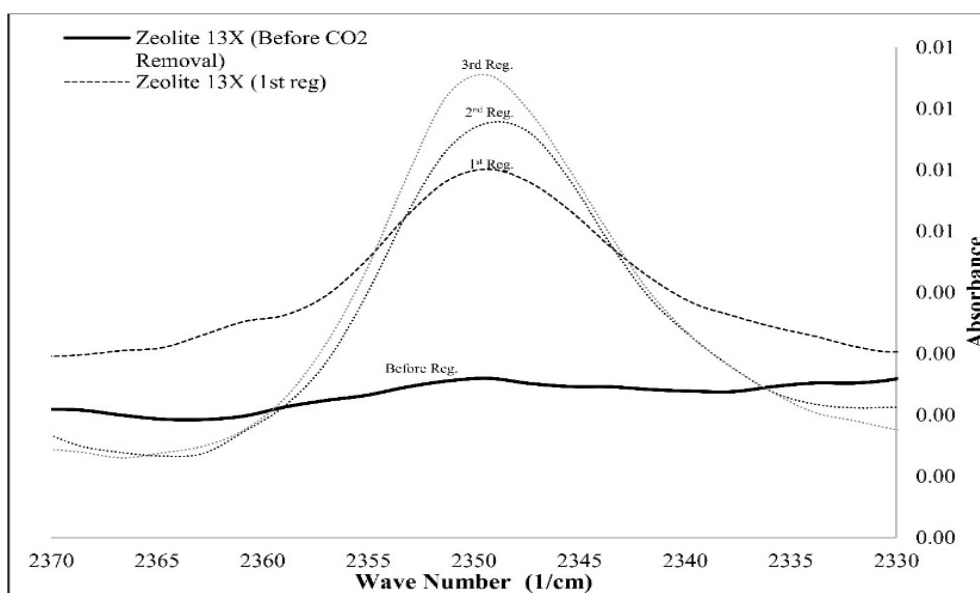


**Figure 10.** FT-IR spectra of the species arising from  $\text{CO}_2$  adsorption on molecular sieve/zeolite 13X (zoomed to  $2330\text{--}2370\text{ cm}^{-1}$ ).

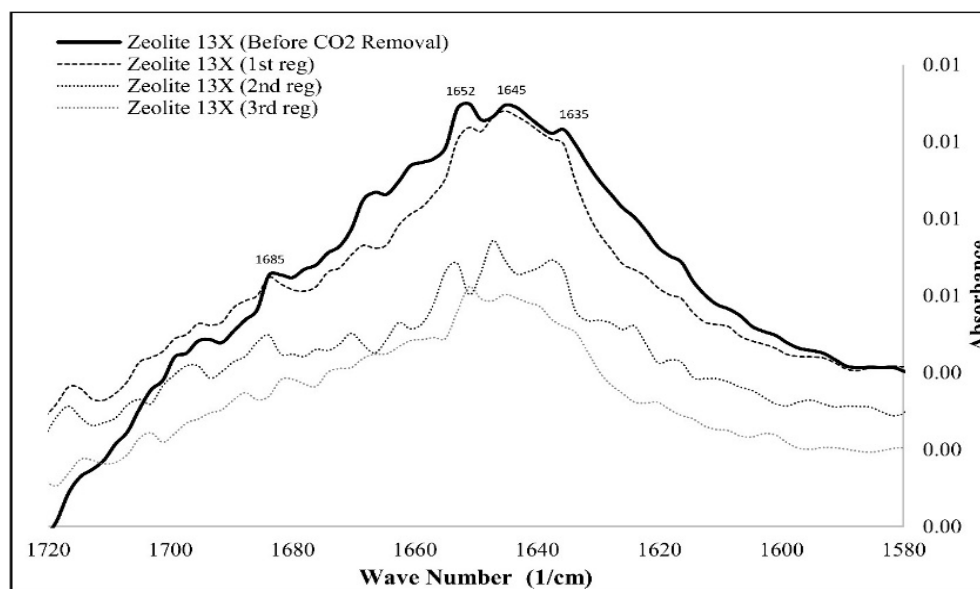


**Figure 11.** FT-IR spectra of the species arising from  $\text{CO}_2$  adsorption on molecular sieve/zeolite 13X (zoomed to  $1580\text{--}1720\text{ cm}^{-1}$ ).

In Figure 10 and 11, the spectra of the surface species arising from CO<sub>2</sub> adsorption on the 13X zeolite adsorbent covered with water are reported. In contact with CO<sub>2</sub> gas, a very strong band reaching saturation of the signal is observed, centered in the region near 2350 cm<sup>-1</sup>. Upon out gassing, the band appears quite symmetrical, centered at 2349 cm<sup>-1</sup>. The position of this band is slightly shifted upwards with respect to the position of the asymmetric OCO stretching of gaseous CO<sub>2</sub>. The shift up agrees with the molecular coordination of CO<sub>2</sub> through one of the oxygen atoms, with retention of the linearity of the molecule. It has been shown that the shift upwards of this vibrational mode roughly depends on the Lewis acidity of the adsorbing center<sup>14</sup>.

Relatively strong bands also form at lower frequencies. In particular, a couple of bands are evident at 1690 and 1420 cm<sup>-1</sup>, together with a negative peak in the subtraction spectrum centered near 1650 cm<sup>-1</sup>, due to the scissoring mode of water that is decreased in intensity upon the admission of CO<sub>2</sub>. The two positive bands correspond well with the two peaks observed in the Raman spectrum of aqueous bicarbonate ion. We can note that this spectrum is significantly different from that of bicarbonate ion adsorbed on the surface of hydroxylated oxides such as alumina<sup>15</sup>. In this case, the symmetric stretching component is observed at higher frequencies, near 1460 cm<sup>-1</sup>, as a result of the coordination of the bicarbonate ion in a bidentate or chelating form. These data strongly suggest that carbon dioxide adsorbs mainly in the form of bicarbonate ion mostly interacting with adsorbed water in the NAX cavities.

Out gassing allows the slow but complete disappearance of the bands of both molecularly adsorbed CO<sub>2</sub> and of bicarbonate ion. Only the formation of a weak sharp component at 2350 cm<sup>-1</sup> can be noticed, intermediately, showing a second type of more strongly adsorbed molecular carbon dioxide.

Some of the low-frequency bands increase in intensity, while bands of molecularly adsorbed CO<sub>2</sub> decrease strongly together with a band at 1645 cm<sup>-1</sup>, possibly associated with traces of water fed as moisture with CO<sub>2</sub>. Although detailed and reliable assignments of these

bands need more investigation, the behavior suggests that these bands can be grouped in several pairs. A quite strong couple of bands growing upon out gassing at 1490, 1435 cm<sup>-1</sup> is assignable to monodentate carbonates. Bands observed at 1760, 1370 cm<sup>-1</sup>, also growing upon out gassing, can traditionally be assigned to “organic-like” or “covalent” carbonates, but are most likely due to “strongly perturbed” bent CO<sub>2</sub> molecules<sup>16</sup>. The position of these bands is similar to that observed for bent CO<sub>2</sub> metal complexes. The shoulders at 1685, 1367 cm<sup>-1</sup> could be due to similar species or to bicarbonate species, while the band at 1581 cm<sup>-1</sup>, stable to out gassing, might be associated to another component in the 1450-1350 cm<sup>-1</sup> range, and attributed to stable bidentate or chelating carbonate species.

By repeating for several times (regeneration cycles), no significant variations are found showing that, at one day's timescale, no significant deactivation of the adsorbent was observed.

#### 4. Elemental (C, H, N, and S content) Analysis after Repeated Cycles of Adsorption

In order to confirm the stability of the zeolite 13X, particularly the stability of the adsorbent on the regeneration by countercurrent of air on the zeolite matrix, adsorption cycles were repeated three (3) times. C, H, N and S analysis was carried using the elemental analyzer, and the samples collected after each adsorption cycle, and the results are given in Table 9.

It was observed that the carbon content initially increased after the 1<sup>st</sup> regeneration and then stabilized at 0.31%. This may be due to some irreversible adsorption of CO<sub>2</sub>, resulting in the possible formation of carbonates. A decline was observed in the hydrogen and nitrogen content of the adsorbents after 1<sup>st</sup> regeneration. The carbon content was largely the same after 2<sup>nd</sup> and 3<sup>rd</sup> regeneration, at about 0.31%, and whereas, for nitrogen, it was about 0.31%. This indicates that some of the loss of CO<sub>2</sub> has been taken place in the 1<sup>st</sup> regeneration

**Table 9.** Elemental analysis of the molecular sieve/zeolite 13X adsorbent

| Sample                         | Nitrogen Content (%) | Carbon Content (%) | Hydrogen Content (%) | Sulfur Content (%) |
|--------------------------------|----------------------|--------------------|----------------------|--------------------|
| Before CO <sub>2</sub> Removal | 0.014                | 0.210              | 1.261                | 1.249              |
| After 1 <sup>st</sup> Reg.     | 0.042                | 0.253              | 1.771                | 1.473              |
| After 2 <sup>nd</sup> Reg.     | 0.024                | 0.311              | 1.332                | 1.192              |
| After 3 <sup>rd</sup> Reg.     | 0.021                | 0.317              | 1.550                | 1.561              |

and further loss was observed in 3<sup>rd</sup> regeneration cycles (dried zeolites).

## 5. Conclusion

The results of the PSA experiments showed an average increase of 160% in the net heating value over that of certified gas standard. The amount of methane was also significantly higher although the amount of the other gasses (i.e. nitrogen) remained comparatively the same. The amount of carbon monoxide was significantly lower and no trace of carbon dioxide was observed in the PSA product gas indicating that carbon dioxide had been completely absorbed by the system. The raw gas inlet flow rate started at 0.71 LPM and ended at around 0.80 LPM until the vessel was regenerated in a countercurrent of air. Based on the product gas composition during the adsorption and desorption cycles, the desired concentration of the product gas was achieved in a short span of 1 minute during adsorption. A longer stable gas concentration may be achieved by using more adsorbent. As the adsorbent became saturated early, using a larger scale PSA system could address the problem. Having two additional PSA vessels would eliminate the product gas concentration cycle and produce a constant desired product gas concentration. With these limitations, however, the use of the PSA system presents a feasible application to producing a cleaner biogas and reducing the problems in downstream activities.

## 6. References

1. Rollo EPF, Pabilona LL, Magomnang AASM, Villanueva EP, Magomnang DMM. Analysis of biogas production from cow chicken and swine manure. *Mindanao Journal of Science and Technology*. 2017; 130-6.
2. Harasimowicz M, Orluk P, Zakrzewska-Trznadel G, Chmielewski AG. Application of polyimide membranes for biogas purification and enrichment. *Journal of Hazardous Materials*. 2007; 144(3):698-702. Crossref.
3. Wellinger A, Lindberg A. Biogas upgrading and utilization. IEA Bioenergy Task 24-Energy from Biological Conversion of Organic Waste. 2001; 1-20.
4. Santos MPS, Grande CA, Rodrigues AE. Pressure swing adsorption for biogas upgrading. Effect of recycling streams in pressure swing adsorption design. *Industrial and Engineering Chemistry Research*. 2011; 50(2):974-85. Crossref.
5. Hauchhum L, Mahanta P. Carbon dioxide adsorption on zeolites and activated carbon by pressure swing adsorption in a fixed bed. *International Journal of Energy and Environmental Engineering*. 2014; 5(4):349-56. Crossref.
6. Maglinao AL, Capareda SC, Nam H. Fluidized bed gasification of high tonnage sorghum cotton gin trash and beef cattle manure evaluation of synthesis gas production. *Energy Conversion and Management*. 2015; 105:578-87. Crossref.
7. Merel J, Clause M, Meunier F. Carbon dioxide capture by indirect thermal swing adsorption using 13X zeolite. *Environmental Progress and Sustainable Energy*. 2006; 25(4):327-33. Crossref.
8. Siriwardane RV, Shen MS, Fisher EP, Poston JA. Adsorption of CO<sub>2</sub> on molecular sieves and activated carbon. *Energy and Fuels*. 2001; 15(2):279-84.

9. Konduru N, Lindner P, Assaf-Anid NM. Curbing the greenhouse effect by carbon dioxide adsorption with zeolite 13X. *AIChE Journal*. 2007; 5(12):3137-43. Crossref.
10. Silva JAC, Schumann K, Rodrigues AE. Sorption and kinetics of CO<sub>2</sub> and CH<sub>4</sub> in binder less beads of 13X zeolite. *Microporous and Mesoporous Materials*. 2012; 158:219-28. Crossref.
11. Jadhav PD, Chatti RV, Biniwale RB, Labhsetwar NK, Devotta S, Rayalu SS. Monoethanol amine modified zeolite 13X for CO<sub>2</sub> adsorption at different temperatures. *Energy and Fuels*. 2007; 21(6):3555-9. Crossref.
12. Montanari T, Finocchio E, Salvatore E, Garuti G, Giordano A, Pistarino C, Busca G. CO<sub>2</sub> separation and landfill biogas upgrading a comparison of 4A and 13X zeolite adsorbents. *Energy*. 2011; 36(1):314-9. Crossref.
13. Beta IA, Hunger B, Bohlmann W, Jobic H. Dissociative adsorption of water in CaNaA zeolites studied by TG, DRIFTS and <sup>1</sup>H and <sup>27</sup>Al MAS NMR spectroscopy. *Microporous and Mesoporous Materials*. 2005; 79(1-3):69-78. Crossref.
14. Nxumalo LM, Ford TA. The Fourier transform infrared spectrum of the boron trifluoride-carbon dioxide complex. *Journal of Molecular Structure*. 1997; 436:69-80. Crossref.
15. Busca G. Bases and basic materials in industrial and environmental chemistry a review of commercial processes. *Industrial and Engineering Chemistry Research*. 2009; 48(14):6486-511. Crossref.
16. Gibson DH. Carbon dioxide coordination chemistry metal complexes and surface-bound species. What relationships? *Coordination Chemistry Reviews*. 1999; 185:335-55. Crossref.